Chapter 9
Mass Spectrometry Techniques in the Analysis of Bioaerosols: Development and Advancement

Rabih E. Jabbour, Samir V. Deshpande, A. Peter Snyder and Mary M. Wade

Introduction

Bioaerosols are airborne particles that may contain pathogenic species, that can cause serious risks to various government and public sectors. The major health concern due to bioaerosols is that certain communicable diseases are transmitted through airborne particles, including viruses, bacteria, and fungi. Moreover, biological warfare agents can be disseminated as bioaerosol particles and could pose severe safety issues for military operations as well as serious economic and health concerns to the public. It had been estimated that when 100,000 persons are exposed to bioaerosol, it would cost approximately $ 26 billion in decontamination and medical treatment [10, 32]. Thus, it is imperative to develop and implement real-time detection and accurate identification technologies for the monitoring of bioaerosols. Initially, bioaerosol analysis was mainly based on traditional microbiological methods involving collection and culturing followed by agar plate counting and often susceptibility tests to antibiotics and microbial phages [57]. Moreover, newly developed molecular biology techniques are being utilized for bioaerosol analyses such as immunoassay, polymerase chain reaction (PCR) amplification, and other gene-based techniques. Although microbiological methods showimpressive sensitivity, they are time- and labor-intensive for sample preparation and analysis, sensitive to shelf life time of the reagents, and beholden to the availability of specific reagents.

Alternatively, several mass spectrometry (MS) techniques have been developed and improved in their sensitivity, fieldability, and compatibility to bioaerosol analysis and characterization in real-time settings, and these have shown promising capabilities. Pyrolysis MS techniques were initially used for analyses in which the bioaerosol particles were heated and their volatile molecules exposed to electron

R. E. Jabbour (✉) · A. P. Snyder · M. M. Wade
U.S. Army Edgewood Chemical Biological Center,
Aberdeen Proving Ground, MD, 21010-5424, USA
e-mail: rabih.e.jabbour.civ@mail.mil

S. V. Deshpande
Science and Technology Corporation, Edgewood, MD, 21040, USA

P. Jonsson et al. (eds.), *Bioaerosol Detection Technologies,* Integrated Analytical Systems,
DOI 10.1007/978-1-4419-5582-1_9,

ionization or chemical ionization, followed by mass spectral detection to establish biomarkers for bacterial differentiation [24, 51–53]. Concurrently, the development of laser desorption–ionization, matrix-assisted laser desorption–ionization (MALDI) [14, 69], and electrospray ionization (ESI) coupled with MS [11, 14, 36, 69, 70] made it possible to analyze large biomolecules such as proteins and oligonucleotides in bioaerosol particles that resulted in enhanced selectivity and identification accuracy. Moreover, several fielded studies showed that MS-based techniques are capable of detecting single bioaerosol particles [25, 27].

This chapter will address the characteristics of various MS techniques used in bioaerosol analysis. An overview of bioareosol MS is presented to provide general perspectives on the application of MS in bioaerosol detection and identification. Also, the capabilities of MS techniques and the nature of their output and impact on the detection and identification of bioaerosols will be discussed. Exploration of the advantages and drawbacks of the applications for different MS techniques in the analysis of bioaerosols is addressed.

Overview of Bioaerosol MS

Spurny [57], provides a review for the detection of bioaerosols. The analysis of bioaerosol sampling includes the stresses that a particle experiences during the collection process. Major stresses and changes that can occur to a bioaerosol particle during the collection includes desiccation; loss of viability due to radiation, oxygen, ozone, prehumidification, or high water vapor concentration; and temperature. These stresses affect the phospholipid, protein, and nucleic acid components of bacteria. Bulk and individual particle interrogation may be performed depending on the analysis technology.

The information content from data reduction of a bioaerosol MS analysis depends on whether the bioaerosol is collected in bulk, as individual particles, or captured in liquid with subsequent sample analysis. Bioaerosols must be converted into a vapor state prior to entrance into a mass spectrometer. The primary method used to accomplish this is pyrolysis or heating of the solids [55]. The solid sample can be either in bulk [25, 27] or individual particle form [51–53]. Both require heating to break up the solid into individual molecules in order to be analyzed by MS. A hot filament, Curie point wire, heated tube, ribbon filament, and laser are the major methods used to heat a solid substance [9, 56]. The tube and wire methods can be performed either without or with derivatization reagents applied directly to the sample prior to heating [1, 2, 12, 13, 25, 27]. A derivatization reagent is necessary if gas chromatography (GC) is part of the MS analysis. The derivatization reagent reacts with acid and alcohol functional groups on compounds to produce esters and ethers, respectively, so as to provide better volatility to very low vapor pressure biochemicals resident in or extracted from bacteria [1, 12, 13, 28].

Bulk bioaerosols usually are deposited in microgram amounts [27]. MS can analyze bulk amounts [25, 27] as well as single particles [24, 51–53, 26] of bioaerosols depending on the interface configuration. However, both sample forms need to be vaporized by a pyrolyzer device (*vide supra*). Another separation technique prior to a mass spectrometer, such as GC or liquid chromatography (LC), requires bulk or microgram amounts in order to provide for enough substance to pass through the column. Single bioaerosol particles need to be vaporized inside the MS vacuum chamber by impacting onto a heated surface prior to analysis. Alternatively, single particles can be vaporized by a laser beam situated perpendicular to the aerosol beam with appropriate triggering mechanisms. Laser pyrolysis features very high heating rates, and single particles can be detected at approximately 10^{-12} g. An early version of this heating technology was called laser microprobe mass analyzer (LAMMA). Single particles were captured in a vacuum ion trap and visually observed with a microscope. A laser beam was positioned to pyrolyze the particle and was analyzed by time-of-flight (TOF)-MS. A limitation in single particle analysis by MS (PAMS) systems is the fact that heating or pyrolysis vaporization techniques generally produce masses of only a few hundred Daltons. Differences in the spectra from different bacteria were not significant, and multivariate data analysis methods are virtually mandatory for pyrolysis of complex substances such as bacteria [7, 8, 39, 66, 68].

Particle Analysis by MS (PAMS)

Biological compounds and substances by definition are associated with very large molecular weight material outside of the detection range of a mass spectrometer, especially when the biomaterial is an intact bacterial cell. Therefore, the key to an analysis is the conversion of the intact cell to small parts, pieces, and components that lie within the range of an MS system. In addition, the initial sample is desired as a stream of aerosol particles.

In the early 1980s, Sinha et al [51–53] adapted the technique of pyrolysis, where a sample was placed on a heated surface such as a filament, boat, or Curie point wire and either slow or rapid heating to 400–500°C produces decomposition of the biological substance into significantly smaller pieces. These pieces usually comprise the fundamental monomer building blocks and fragments thereof. The method, PAMS, produces an aerosol particle beam by simple expansion through multiple skimmers at differentially pumped lower pressure regions to remove the gas load (Fig. 9.1). Isokinetic sampling of the particles allowed for a significant increase in particle transmission to approximately 70% reaching the mass spectrometer with respect to that entering the particle beam tube. The transmitted particles hit a hot vee-shaped rhenium filament in a 10^{-6} Torr ionization source. An electron beam ionizes the hot neutrals, and the ions are extracted into the quadrupole mass spectrometer (QMS). *Pseudomonas putida*, *Bacillus subtilis* (BG), and *Bacillus cereus* were investigated (Fig. 9.2). All three provided very similar mass spectra including

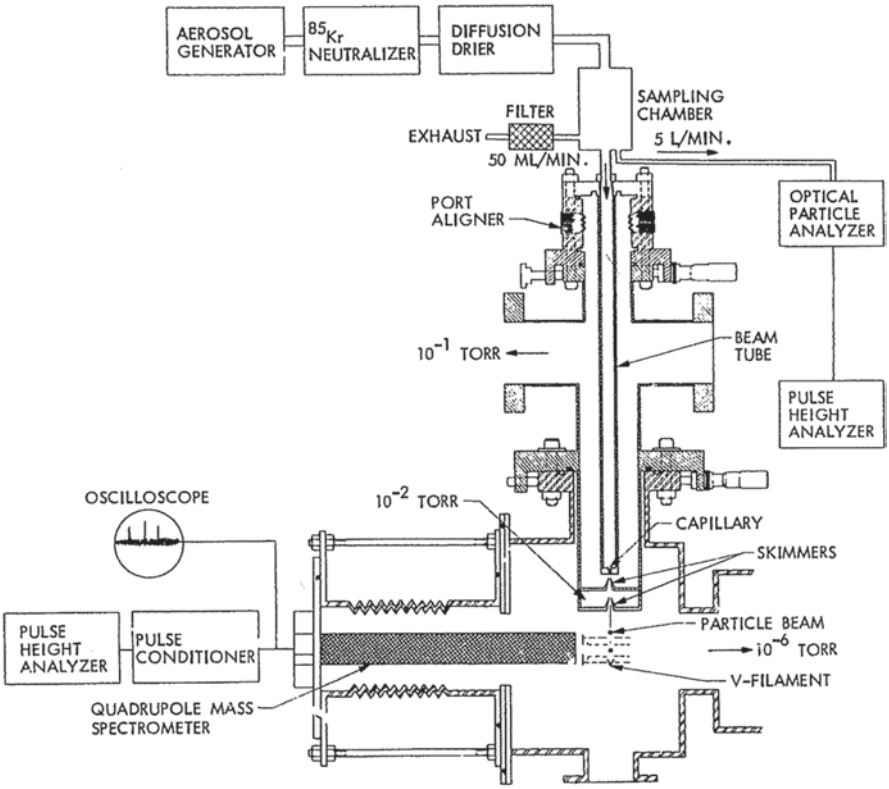

Fig. 9.1 Particle analysis by mass spectrometry (PAMS) system. (Reprinted with permission from Sinha et al. [52]. Copyright 1984 Elsevier Science Publishers B.V., Amsterdam)

a small peak at m/z 282 and masses of less than m/z 169. This work provided the first evidence for MS analysis of beams of bacterial particles.

Early Bioaerosol Ion Trap MS

Gieray et al. [24] extended the work by Sinha et al. [51–53] in that the QMS was replaced with an ion trap tandem mass spectrometer. Five different bacteria were used for bioaerosols. Mass spectra were characterized as a peak at every mass, and masses were observed up to m/z 220 in the positive ion mode. Figure 9.3 shows mass spectra for *Enterobacter aerogenes*, BG, and *Micrococcus lysodeikticus*. Individual bacterial particles produced considerable variations from cell to cell, that is, spectrum to spectrum. The variations included total number of peaks and peak height ratios. Space charge saturation of the ion trap usually occurred, and this can represent a cause of poor spectral resolution and reproducibility. Negative ion spectra resulted in masses up to m/z 300.

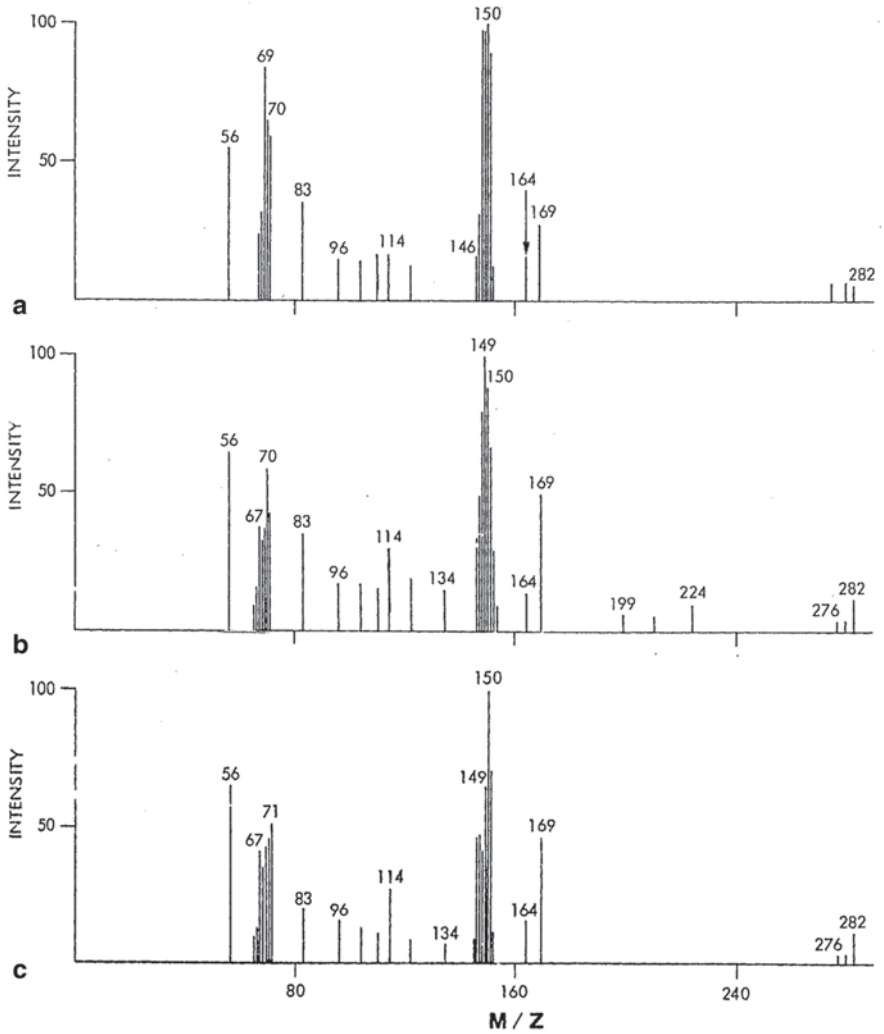

Fig. 9.2 Mass spectra of particle analysis by mass spectrometry (PAMS) system of particles of (**a**) *Pseudomonas putida*, (**b**) *Bacillus cereus*, and (**c**). *Bacillus subtilis*. (Reprinted with permission from Sinha et al. [52]. Copyright 1984 Elsevier Science Publishers B.V., Amsterdam)

Bioaerosol Matrix-Assisted Laser Desorption–Ionization Time of Flight Mass Spectroscopy

Initial Studies

In the mid-1990s, Murray and Russell provided a series of papers showing that the MALDI-TOF-MS technique could analyze a stream of aerosols. The core principle of MALDI is that a solid or liquid sample analyte is mixed with one of a series of

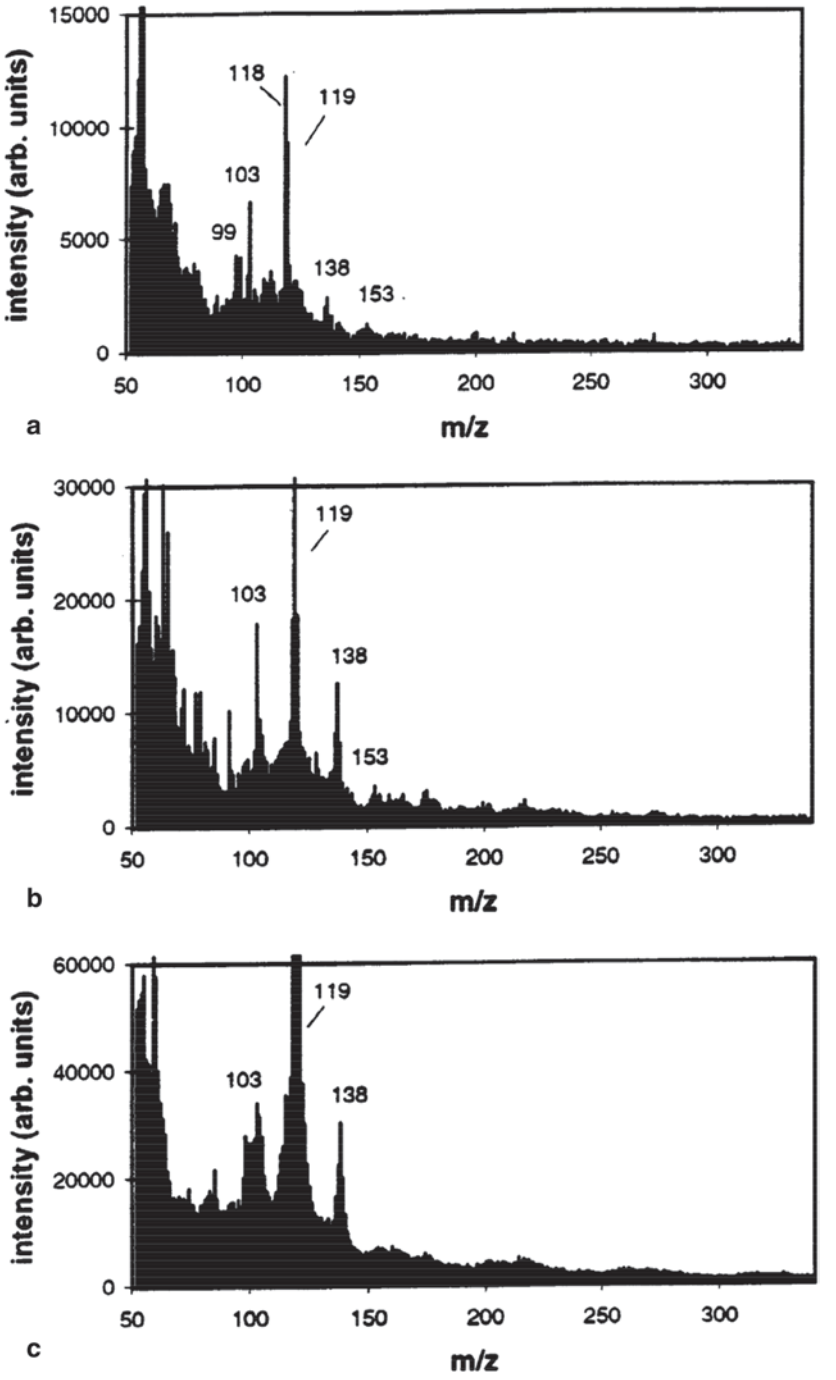

Fig. 9.3 Laser ablation ion trap positive ion mass spectra of (**a**) *Enterobacter aerogenes*, (**b**) *Micrococcus lysodeikticus*, and (**c**) *Bacillus subtilis* var. *globigii*. (Reprinted with permission from Gieray et al. [24]. Copyright 1997 Elsevier Science Publishers B.V., Amsterdam)

aromatic functional group-containing chemicals or matrices. A portion is placed on a support and inserted into the vacuum chamber of an MS system, and a laser impinges on the surface to "lift" or vaporize the sample as well as ionize the sample.

Significantly, Murray and Russell [41] also showed that a mixture of matrix and sample can be aerosolized. The liquid enters the nebulizer at up to 1 mL/min, and the aerosol particles are initially wet. Therefore, the particles had their solvent adduct molecules removed as the particles passed through a drying tube. A desolvation gas stream also helped dry the particles. The released solvent and carrier gas were removed with high-speed pumps prior to particle introduction into the TOF-MS vacuum. The particle beam was collimated, and a perpendicular ultraviolet (UV) laser beam ablated and ionized the particles. The ions were directed into and analyzed by a TOF-MS system [41]. Fundamental parameters were investigated and compared to the surface, bulk MALDI procedure. Investigations included matrix to analyte ratio, performance of different organic matrix ion yield at different laser energies, and intensity with respect to the temperature of the drying tube. The size of the matrix-covered particle also was analyzed.

The particle size did not depend on the amounts of matrix or analyte mixed together or the matrix substance. The length of the drying tube did have an effect where a 6 or 25 cm tube length produced 50 and 100 μm-sized aerosol particles, respectively. With the 25 cm tube, the particle size did not vary from 25 to 500 °C drying tube temperature. Thus, it appeared that the drying gas was a more important parameter compared to the tube temperature for final particle size characterization.

Aerosols of a mixture of analyte–MALDI matrix started with bovine insulin as a test compound [41]. The concentration of matrix and protein analyte was investigated in order to obtain a good signal to noise ratio (S/N). Two considerations were addressed, namely the prevention of nozzle clogging and matrix–analyte ratio. It was found that ~2 mg/mL each of 4-nitroaniline matrix and bovine insulin protein were the highest amounts that could be used without clogging the nebulizer orifice and for satisfactory ion intensity. A minimum ratio of matrix and analyte was about 50 : 1 to prevent clogging the aerosol orifice. Note that for regular surface MALDI, matrix and analyte amounts span the 100–50,000 ratio range.

Several matrices were also investigated and the α-cyano-4-hydroxycinnamic acid (CHCA) matrix provided an M^+intensity of bovine insulin 12× higher than that of the 4-nitroaniline. However, the M^+signal was very broad compared to 4-nitroaniline. Therefore, 4-nitroaniline was deemed as the best compromise matrix.

General comparisons were made to surface MALDI. Compared to the surface version, aerosol MALDI has a (a) lower mass resolution, (b) higher limit of detection, (c) mass peak range <300 Da, and they mostly arose from protonated and alkylated solvent clusters and not the matrix, (d) better performance with a lower matrix to analyte ratio, and (e) better S/N with higher laser irradiance.

The following provides a summary of improvements and refinements in the bioaerosol MALDI technique. This development consisted of transforming the exit of an LC column into an aerosol spray [40]. Prior to the exit, the LC effluent of a protein mixture was mixed with a matrix solution in a mixing tee. The matrix–analyte mixture subsequently entered the nebulization chamber at a rate of 0.5–1.0 mL/min

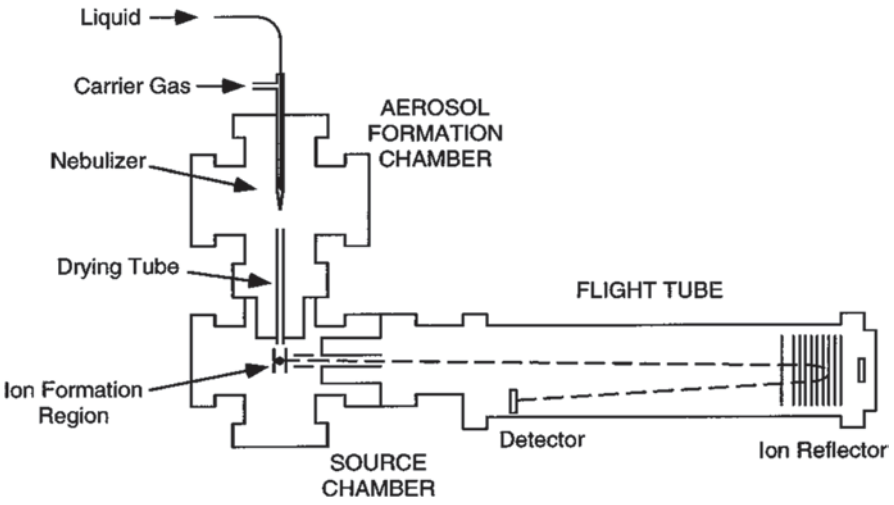

Fig. 9.4 An aerosol matrix-assisted laser desorption–ionization (MALDI) reflectron time-of-flight (TOF) mass spectrometer. Aerosol particles are formed in the vacuum chamber and passed through a heated drying tube into the ion source. The laser vaporizes the individual particles and forms ions. The ions are accelerated into the MS detection chamber. (Reprinted with permission from Fei et al. [16]. Copyright 1996 American Chemical Society)

and sprayed toward the entrance of a TOF-mass spectrometer. Analytes consisted of a mixture of nanomole concentrations of bradykinin, gramicidin S, and myoglobin. A three-dimensional (3D) retention time–flight time plot revealed the three distinct protein peaks.

Reflectron Time of Flight Mass Spectroscopy

Aerosol-MALDI still had some challenges such as the relatively large amounts of sample needed for satisfactory detection and mass resolution. A continuous aerosol beam necessarily uses a relatively large amount of sample. Even though only femtomole amounts of sample were actually ionized, hundreds of nanomoles of biological substance were expended. Using a mixture of bradykinin, angiotensin II, gramicidin D peptides, and vitamin B_{12} [16], improvements were made in aerosol-MALDI-TOF-MS. Mass resolution was a problem, and it was reasoned that thelinear TOF-MS be replaced with a reflectron TOF-MS system. A reflectron takes into consideration the spread of ion energies. The higher energy ions follow a longer drift tube flight path to reach the ion detector with respect to the lower energy ions (Fig. 9.4). A reflectron causes the ions to have the same energy. This allows them to arrive at the detector at the same time and therefore increases the signal strength that is manifested by a sharper peak in the mass spectrum. Mass resolution of the bradykinin, angiotensin II, and gramicidin D ions were 270, 330, and 310, respectively (Fig. 9.5). Earlier work [41, 42] produced a resolution on the

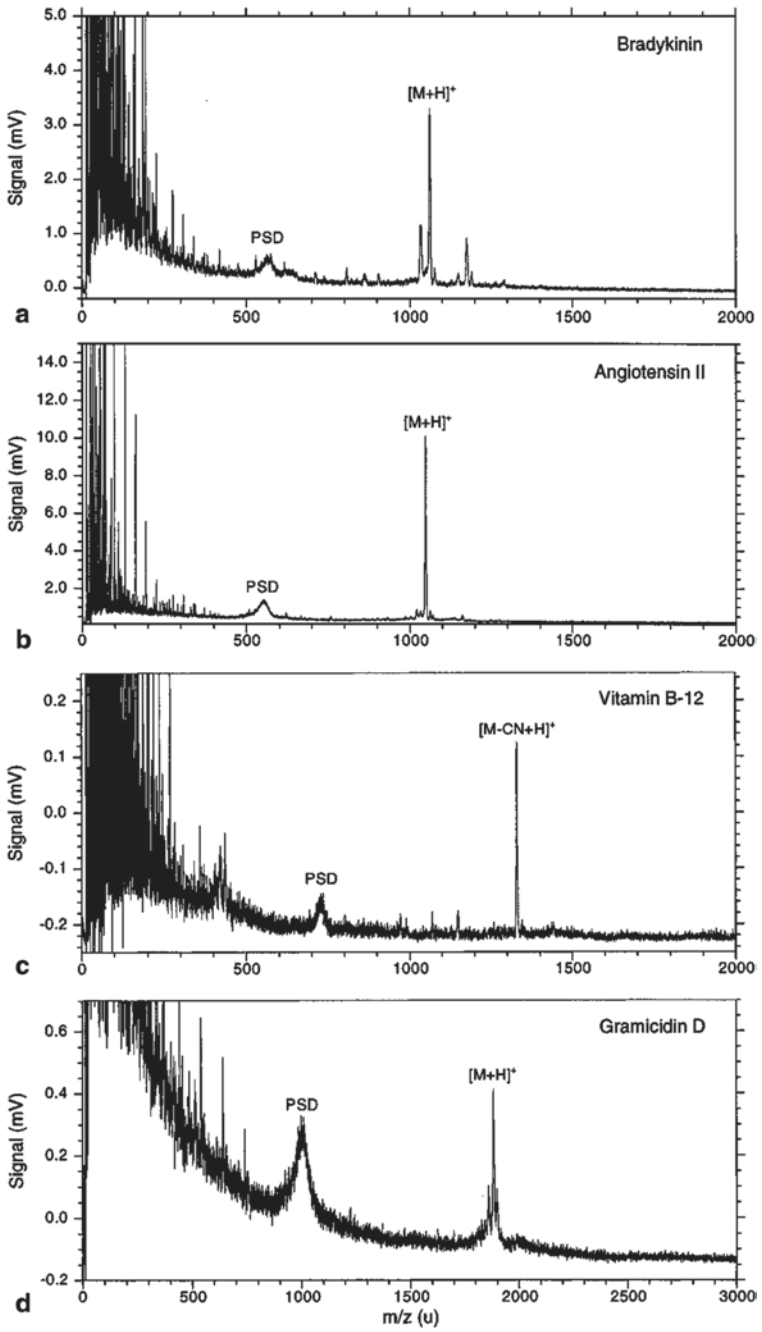

Fig. 9.5 Mass spectra from the MALDI reflectron of (**a**) bradykinin peptide, (**b**) angiotensin II, (**c**) gramicidin D, and (**d**) vitamin B_{12}. (Reprinted with permission from Fei et al. [16]. Copyright 1996 American Chemical Society)

order of only six for bovine insulin. A reflectron greatly improved mass resolution of peptides and proteins. The mass resolution was highest at 440 m/Δm when the laser energy was at a value of 10 mJ, which was the lowest energy above the threshold of ion appearance. Resolution decreased to approximately 300 for laser energies at 200 mJ for the peptides. The 300–400 resolution values are >10× that for aerosol MALDI-linear TOF.

Salient information on mass resolution includes the time duration of ion formation, initial ion spread in space, and ion source pressure. A reflectron can compensate or provide path lengths such that all the ions result in similar energies. The initial ion energies can be 10–20% in variance. The laser itself causes an approximate 6% energy spread of isobaric ions. Thus, it appears in a practical sense that the spread of ions is not the limiting cause of mass resolution. However, ion-neutral collisions in the laser ionization region can cause a distribution of energies, which is not taken into consideration in the 6% energy spread approximation from the laser itself. This ion spread causes the $[M+H]^+$peak to widen.

Ionization Efficiency

Mentioned earlier was the overwhelming amount of gas (pressure) found when nebulizing a liquid such as a mixture of analyte and MALDI matrix [3]. Excess gaseous material was pumped away prior to the ion source since this excess neutral gas species can cause considerable problems for efficient ion resolution in the mass spectrometer. Ion-neutral collisions cause nonuniform ion energies, and it introduces a spatial spread of ions. The latter deteriorates the focusing of the ions. These are functions of the ion yield, and further work was performed to refine the analyte concentration and matrix to analyte ratio with respect to their earlier work [16, 40–42]. A mixture of bradykinin and gramicidin S peptides and bovine insulin and myoglobin proteins were used [3]. A bioaerosol particle includes the biological analyte as well as salt, buffer, trifluoroacetic acid modifier, organic matrix, and residual solvent species. These compounds can affect the ionization efficiency of the biological analyte component and provide excess neutral molecule presence to destabilize the ion current, broaden peak widths, and reduce detection efficiency. It was shown that the ion signal for aerosol MALDI was nonlinear with respect to the analyte concentration, and this was attributed to residual solvent in the particles [3]. With increasing particle size, it was shown that solvent content increased causing a decrease in ion signal. Evidence also suggested that the presence of solvent in the aerosol particles did not affect the ionization efficiency in a uniform manner for different matrices and analytes. In order to overcome this problem, it was suggested that internal standards mixed in with the aerosol process may be required.

Three significant points for bioaerosol MALDI were observed: (a) matrix–analyte ratios for optimal ion yield were 10–100 : 1, (b) desolvation or removal of solvent to produce drier particles allowed for greater biological analyte ion signal, and (c) sensitivity was analyte dependent. Based on the number of residues, hydropho-

bicities, and surface area of each analyte, a correlation was established between particle size and ionization efficiency.

A similar effect for online bioaerosol matrix particle generation was performed by Mansoori et al. [38] where the dried droplets exiting the heated particle drying tube were ablated and ionized in flight with subsequent ion extraction into a TOF-MS system. Leucine enkephalin and gramicidin S were used for the analyses. Improvements implemented were a uniform size, shape, and composition of the monodispersed aerosol compared to the heterogeneous (or polydisperse) distribution of these parameters for aerosol particles [3, 16, 40–42]. Further, light scattering was used to detect each particle so as to trigger the laser to ablate the matrix-coated analyte for on-line MALDI. 3-nitrobenzylalcohol (3-NBA, liquid) and 2,5-dihydroxybenzoic acid (DHB, solid) were the matrices used. Intense $[M–H+2Na]^+$peaks were observed. The threshold for ionization of leucine enkephalin was approximately 0.2 mJ. Up to 2 mJ of laser energy or fluence provided only a minimal increase in the $[M+Na]^+$signal area. This was most likely due to the monodisperse, uniform nature of the particles at 4.7 μm. Gramicidin S also displayed $[M+Na]^+$ions.

Matrix Coating of Bioaerosol in the Vapor Phase

In the early 2000s, two other methods were devised by a pair of research groups to advance bioaerosol MALDI [30, 31, 33, 62]. In one of the developments [30], particles entered a chamber containing a heated, saturated vapor of organic matrix. As the aerosol penetrated the vapor in the chamber, the matrix condensed on the analyte particles. The matrix-laden particles exited the chamber and were collected on a surface for 5 min. Laser impingement created the ions for TOF-MS analysis. This process resulted in an off-line aerosol MALDI-TOF-MS method [30, 33].

In the work by Jackson and Murray [30], size distributions of particles were investigated with and without matrix vapor in the saturation container, and these two conditions caused the mean of the mass-weighted particle size distribution to decrease from 1.54 to 1.34 μm, respectively. Gramicidin S and gramicidin D peptides with 3-NBA matrix were used. As in all the above analyses [30, 31, 33, 62], the M^+, $[M+H]^+$, and alkali adduct M^+ ions were observed.

A 5-min, off-line deposition of picolinic acid (PA)-coated erythromycin produced an intense $[M+Na]^+$ peak at 757 Da and that of the on-line analysis produced no high-mass information [31]. The mass spectra mainly consisted of <200 Da masses. On-line analysis included a container saturated with MALDI matrix vapor for condensation on bioaerosol particles. On-line, single particle analyses proceeded where ions were continuously extracted from the ion source for analysis. On-line aerosol MALDI analysis of NBA-coated erythromycin showed a significantly smaller $[M+H]^+$ peak at 735 Da [31] compared to the same spectral peak for PA. On-line analysis of NBA-coated gramicidin S particles resulted in a relatively small $[M+Na]^+$ peak at 1164.5 Da, while PA matrix did not produce a molecular ion. Off-line analysis of gramicidin D coated with PA matrix resulted in a poor spectrum with significant low mass interference.

Kim et al. [33] presented off-line *Escherichia coli* aerosol MALDI-TOF-MS information. Two matrices, CHCA and sinapinic acid (SA), were used. Three different methods of combining *E. coli* and matrix were investigated with off-line MALDI-TOF-MS analysis. Each of the six aerosol permutation procedures along with the standard dried droplet method (*vide infra*) with both matrices resulted in eight experiments yielding several different distributions of ions shown in figure 9.6a–g in the 3000–10,000 Da range [33]. Mass spectra from the three techniques were compared to that from the standard dried droplet method, which merely is mixing the initially impacted bacteria with a drop of MALDI organic compound (matrix) and subsequent drying. The four methods were as follows:

1. Standard dried droplet method: An amount of *E. coli* bacteria from a suspension was pipetted onto a MALDI target plate. One microliter of saturated liquid matrix was added to the spot and dried. This was performed for both CHCA (Fig. 9.6a) and SA (Fig. 9.6b) matrices. Matrix solution was added to the dried bacteria to produce the MALDI phenomenon. The deposited bacteria required the matrix solution to be added to produce the MALDI phenomenon (Figs. 9.6a, b).
   The mass spectra in Fig. 9.6a, b were used for comparison to the subsequent bioaerosol-generated MS in Fig. 9.6c–i. Figure. 9.6a, b shows between 30 and 40 peaks. The CHCA matrix generated many more peaks < m/z 6000 than that for SA. A reproducibility of > 95 % was observed for peaks having an S/N > 3.
2. Bioaerosol method 1: A suspension of lyophilized *E. coli* was aerosolized with a collision nebulizer, and an Andersen impactor was used to collect and concentrate the bioaerosol onto a MALDI target plate. One microliter of saturated liquid matrix was added on top of the spot and dried. This occurred for both CHCA and SA matrices. The impacted dry aerosol required the matrix solution to be added to produce the MALDI phenomenon (Figs. 9.6c, d).
   Figure 9.6c, d resulted from CHCA and SA as organic matrix, respectively. Compared to Fig. 9.6a, b, c, and d were obtained using one-third higher laser fluence to obtain adequate signal above m/z 6000. Fewer peaks are observed for identification utility in Fig. 9.6c, d compared to Fig. 9.6a, b.
3. Bioaerosol method 2: Four hundred microliters of matrix were applied to a MALDI target surface and dried. Afterwards, the bacterial aerosol was impacted directly onto the dried matrix, and 200 μL of a 1 : 1 mixture of acetonitrile—water not added (Fig. 9.6e with SA matrix) and added (Fig. 9.6f (CHCA) and 9.6 g (SA)) to the impacted bioaerosol with subsequent MALDI-MS mass spectral analysis.
   In Fig 9.6e, f, and g *E. coli* aerosols were employed for MALDI analysis. However, the order of deposition onto a solid metal target of matrix and aerosol was reversed from that shown in Fig. 9.6c, d. Figure 9.6e shows no signal > m/z 3000; however, mass spectral signals appeared with the addition of a solvent mixture (Figs. 9.6f, g). Figure 9.6b and g are very similar in appearance. Figure 9.6f is lower in resolution, lower in the number of peaks, and generally of lower quality than that in Fig. 9.6a.

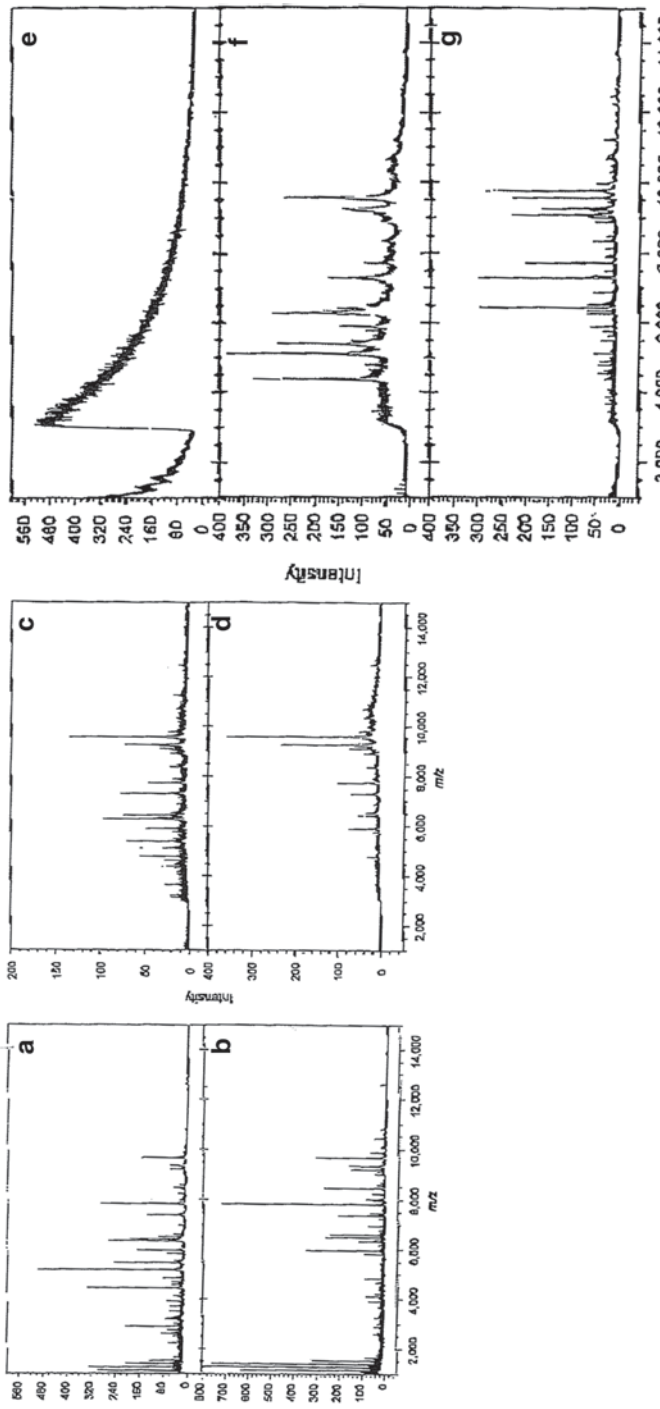

Fig. 9.6 Matrix-assisted laser desorption–ionization (MALDI) time-of-flight mass spectra of *Escherichia coli* bacteria and (**a**) α-cyano-4-hydroxycinnamic acid (CHCA) and (**b**) sinapinic acid (SA) matrices. Mass spectra of *E. coli* by placing 1 μL of (**c**) CHCA and (**d**) SA matrix on top of the collected bioaerosol particles. Mass spectra of bioaerosols deposited on a target surface already coated with (**e**) SA matrix with no additional treatments, (**f**) CHCA matrix and 200 μL of solvent, and (**g**) SA matrix and 200 μL of a 1 : 1 acetonitrile/water solvent. Bioaerosols placed onto a target surface that was precoated with CHCA and SA matrices with a sprayed solution of 1 : 1 acetonitrile/water solvent. (Reprinted with permission from Kim et al. [33]. Copyright 2005 John Wiley & Sons, Ltd.)

4. Bioaerosol method 3: Bioaerosols were impacted onto the MALDI target surface and organic matrix was spray-deposited onto the bacteria. The solvent mixture was then sprayed onto the target by a collision nebulizer and dried. Then MALDI-MS mass spectral analysis then took place (Fig. 9.6f (CHCA) and g (SA)).
   Relatively few peaks are observed in Fig. 9.6f and g compared to Fig. 9.6a–g. The broad mass peaks in Fig 9.6f and g indicate low mass resolution and relatively poor mass spectral fidelity for the bioaerosol method.

The laboratory work [33] presented above has ramifications with respect to translation into field portable and transportable instrument scenarios. Solvents and organic matrices are liquids as well as expendable components. They necessitate reservoirs built into the instrumentation. Pre-coated MALDI solid targets would not be reliable, instead, the matrix and solvent need to be applied to the deposited bioaerosol in a real-time fashion. Therefore, these expendable liquids need to be replaced periodically, and the liquids necessitate an increase in size and complexity of the system.

In another development, Stowers et al. [62] applied a similar online MALDI-TOF-MS concept except with whole bacteria analyte, and the particles were analyzed in real time. That is, triggering was performed and an excimer laser was turned on and off to ablate and ionize the particles in the airstream. This was accomplished by splitting a HeNe laser into two beams perpendicular to the particle stream. The HeNe laser beams detected a particle, and this was used to turn on the excimer laser at the appropriate time to ablate and ionize the particle. BG spores were aerosolized and entered a chamber containing heated, vaporized organic matrix. Matrix coating of the particle took place as it traversed the vapor. Upon exiting the chamber, the aerosol BG particles were ablated and ionized. The ions were focused into a TOF-MS. 3-NBA did not produce signals > 200 Da for BG. PA matrix, however, produced a single peak at 1224 Da, which was tentatively attributed to a portion of the peptidoglycan. That was the only observed peak > 1000 Da.

Harris et al. [26] extended the above on-line aerosol MALDI technique by replacing the TOF-MS with an ion trap MS system (Fig. 9.7). An aerodynamic six lens system was also incorporated prior to the laser ionization source. Matrices PA and 3-NBA were used. Solid matrices were heated and saturated in a condenser where the particles passed through. The vapor phase matrix condensed onto the exterior of each particle to form a coating. Sharp MH^+ bradykinin peaks with NBA and PA matrices were observed for single particles in Fig. 9.8a and b, respectively. Bradykinin was deposited on a probe, and Fig. 9.8c presents an average mass spectrum from 256 separate laser-derived mass spectra. A significant increase in mass spectral peaks was observed with 3-NBA and leucine enkephalin, and the base peaks were MH^+ and $[M+Na]^+$. With the aerodynamic lens and ion trap MS systems, attomole sensitivity was observed for 1 μm particle diameters, which was significantly better than the performance of an aerosol MALDI-TOF-MS [30, 31, 33].

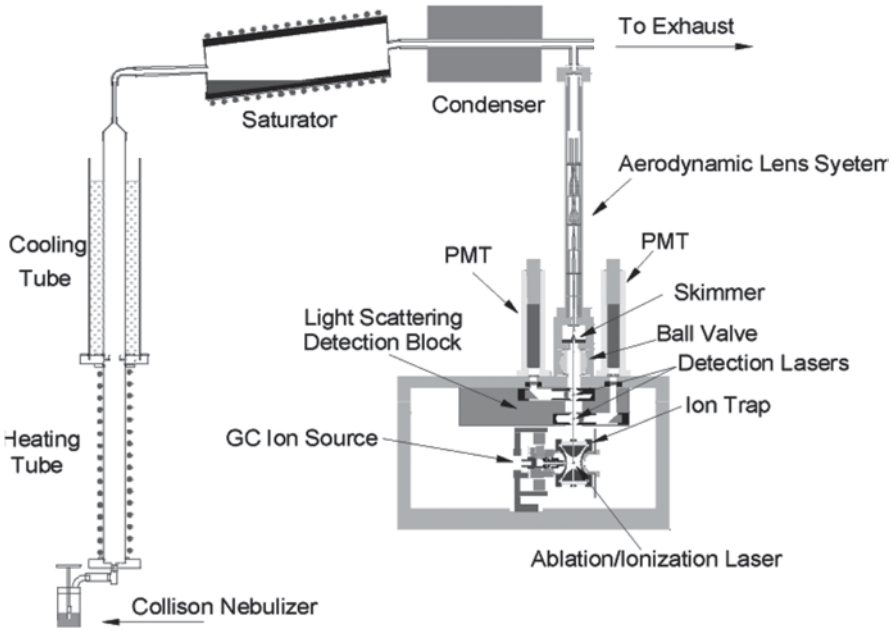

Fig. 9.7 A bioaerosol generator, online organic matrix condensation module onto the aerosol particles, and aerosol ion trap mass spectrometer. (Reprinted with permission from Harris et al. [26]. Copyright 2005 American Chemical Society)

Nanoparticle Bioaerosol

Wilson et al. [67] published information where a system similar to the aforementioned [26] was built, except that a TOF-MS system replaced the ion trap-MS. Test biochemicals included tryptophan and Phe-Gly-Gly biochemicals and no MALDI matrix was used. Instead the pure biochemicals were transformed into nanoparticles and passed through a five-aperture aerodynamic lens system. The particles entered a 10^{-5} Torr ion source. The aerosol impacted onto a heated copper tip and the plume was ionized by a vacuum UV photon beam from a synchrotron (photoionization). Sharp intense M^+ ions (204 Da) were observed at the lowest bioaerosol vaporization temperature of 373 K and 8 eV photoionization energy. Increasing the temperature to 573 K with an 8 eV photoionization energy resulted in essentially the methylene indole fragment, $C_9H_8N^+$, at m/z 130. Vaporization of Phe-Gly-Gly showed an intense M^+ at m/z 279 with essentially no fragmentation at 323 K with an S/N = 800. An observation concerning the use of nanoparticle generated biological compounds is that decomposition of the compounds into small fragments is minimized. A logistic convenience is that a complex system to jet cool the desorbed molecules is not necessary because the desorbed molecules are relatively cool so as to prevent significant thermal decomposition. This internal energy deposition can be controlled so as to vary the amount of decomposition if desired.

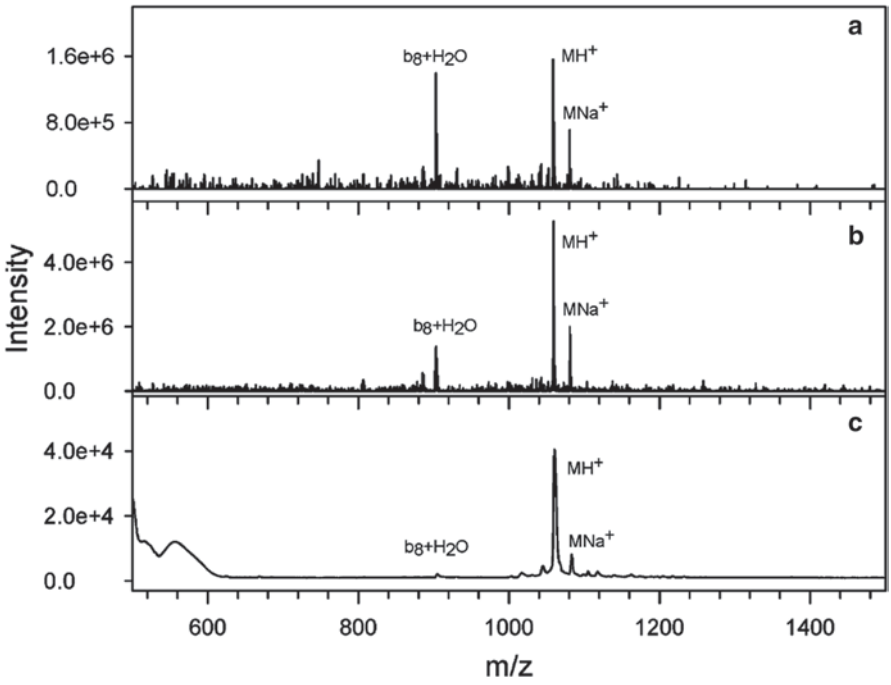

Fig. 9.8 Single-particle MALDI mass spectrum of (**a**) bradykinin coated with 3-nitrobenzyl alcohol, and (**b**) bradykinin coated with picolinic acid; (**c**) MALDI mass spectrum of an average of 256 laser shots performed on separate regions of bradykinin placed onto a probe. (Reprinted with permission from Harris et al. [26]. Copyright 2005 American Chemical Society)

Addition of Ultraviolet Fluorescence Triggering

An improvement was provided with respect to the aforementioned bioaerosol on-line and off-line TOF-MS literature [24, 26, 67]. The improvement consisted of selective MALDI of biological particles as guided by UV fluorescence triggering of those particles [65]. Ferrulic acid was the MALDI matrix and insulin, myoglobin, cytochrome c, and BG organism were the bioaerosols. $[M+H]^+$ ions were observed for the protein analytes in an off-line collection of particles with premixed ferrulic acid and biological substance. This method provides masses of proteins of up to 20,000 Da, which can increase the efficiency of data analysis methods for better identification figures of merit.

Single Particle vs. Bulk Mass Spectra

An interesting situation occurred where the mass spectrum of an aerosol particle of myoglobin and an averaged spectrum of 40 particles were compared [34]. Both spectra had a mass resolution <50 and both $[M+H]^+$ and $[M+2H]^{2+}$ species were

observed at 16,952 and 8477 Da, respectively. Intensities were higher in the averaged spectrum. However, the averaged spectrum had a lower mass resolution. It was expected that an averaged mass spectrum should have better mass resolution than a single-shot spectrum. This can be explained by the different ionization regions for different particles as they travel through the width of the laser beam waist. Different ionization regions mean different ion flight path lengths and hence different ion flight times. Ions generated from surface MALDI do not experience this anomaly.

Single aerosol particles of *Erwinia herbicola* (EH) vegetative cells were investigated by online aerosol TOF-MS. A HeNe fluorescence emission system was used to trigger the 308 nm excimer laser to ablate and ionize the particles. SA was pre-mixed with the bacteria to a 1 mg/mL concentration and dried. The powder was nebulized into the vacuum system, and sharp peaks were observed in the 5000–20,000 Da range.

Bioaerosol Mass Spectrometry

Initial System

A project developed at Lawrence Livermore National Laboratories (LLNL) documented success in tackling the challenge of detection and identification of bacterial aerosols by TOF-MS. The impetus for developing a bioaerosol-TOF-MS system originated in the modification of a system based on the analysis of ambient inorganic and organic aerosols [35, 63] naturally found, generated, and released into the environment. Temporal characteristics of ambient firework pyrotechnic [35] releases were monitored. Combinations of inorganic ions as well as select ambient hydrocarbons were noted. The instrument was called an aerosol TOF-MS system (ATOFMS), and it was used to investigate ambient atmospheric fine (100–300 nm) and ultrafine (< 100 nm) particles consisting of simple organic compounds. Pyrotechnic material that was sampled from the ambient atmosphere included alkali and alkaline ions.

Other ambient analytical challenges [4, 23] included wood smoke, particles containing masses attributed to oxygenated linear hydrocarbons [50] such as aldehydes, and acetonitrile car emissions in an on-line fashion. In the present discussion, microliters of BC, *Bacillus thuringiensis* (BT), and *B. subtilis* variant niger (BG) suspensions were pipetted onto a sample probe and dried. Either an infrared (IR) or UV laser was used to effect ionization.

The bioaerosol-TOF-MS system developed at LLNL does not use matrix, liquid, or solid consumables [46, 59]. In the development of this system (Fig. 9.9), a collision nebulizer provided BG aerosols, and they were dried by passing through a drier desiccant tube. The spores passed through a sizing region consisting of two lasers. A frequency-quadrupled, Q-switched Nd:YAG ablated, desorbed, and ionized each particle. Both positive and negative ions are scanned because two separate TOF-MS tubes emanate 180° from the ion source. The system was called the bioaerosol MS (BAMS) system. Typical mass spectra for a BG spore shows positive ions < 150 Da

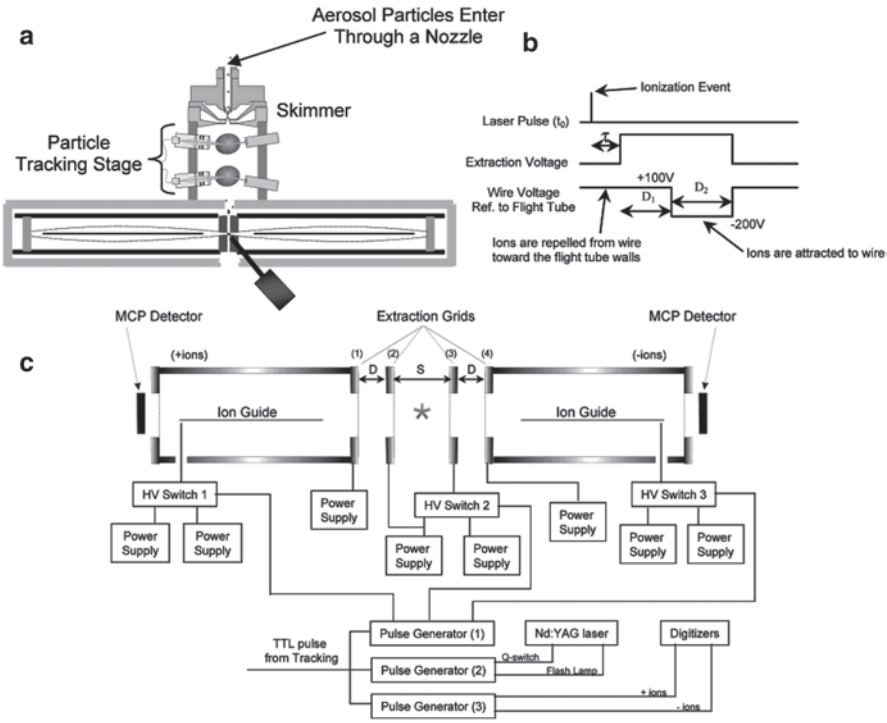

Fig. 9.9 (**a**) Schematic of the bioaerosol mass spectrometry system (BAMS), (**b**) timing diagram of the BAMS for delayed ion extraction and pulsed ion guide wires, and (**c**) schematic of the pulsing and wiring that controls the triggering of the delayed ion extraction and ion guide wires. (Reprinted with permission from Russell et al. [46]. Copyright 2005 American Chemical Society)

and negative ions < 200 Da (Fig. 9.10). This was the first recording of positive and negative ion mass spectra from the same biological particle. In the negative mode, as the laser energy increased, lower numbers of masses appeared, and this trend was reversed in the positive mode. The high mass peak intensities (> 160 Da) increased when the laser energy was increased. Figure 9.10 shows that at relatively low laser energies, very few peaks were observed in the positive mode. At higher laser energies, an increased number of peaks are observed predominately in the low mass range (< 66 Da). It was shown that the laser fluence or energy was a very important variable in the generation of quality TOF mass spectra.

The development of the BAMS [17] saw scrutiny on the concept of analyzing every particle in succession. Spores of BG and BT were used with no liquid reagent. Laser desorption/ionization TOF-MS was reported for aerosols of spores, and rapid data analysis was highlighted. The data analysis starts with a positive and negative mass spectrum of 350 masses (elements) or measurable mass bins for each spectrum. The spectrum was treated as a vector, thus similar spectra are equivalent to similar vectors. In that case, the angle between the two vectors is small. The experimental spectra are then compared to a database of the organism. The positive

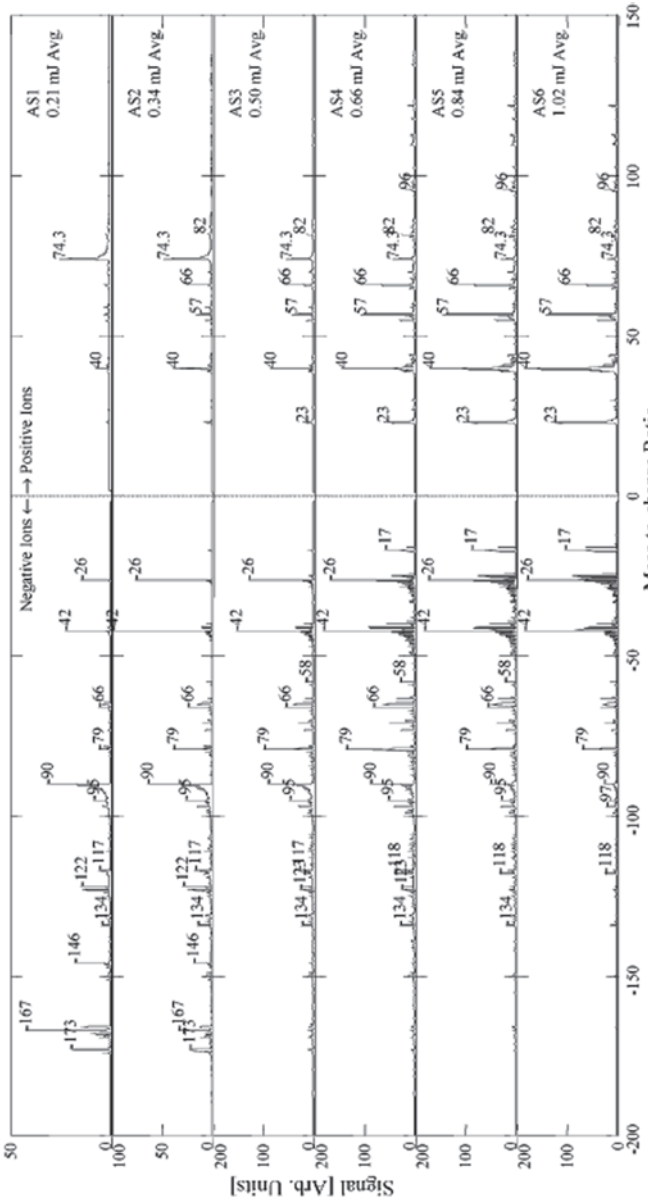

Fig. 9.10 Averages of 1000 spectra (AS) collected at each average laser energy given to the right of each spectrum. The highest intensity mass peaks in the negative ion mode are in AS1 and steadily decrease from AS2 to AS6. The highest intensity mass peaks in the positive ion mode, however, steadily increase and are greatest in AS6. The spectral differences result from changes in the average fluence produced by each laser setting. Therefore, the laser profile must introduce spectral variability from shot to shot since successive spores interact with different regions (and different fluences) in the nonuniform profile and absorb different amounts of energy. (Reprinted with permission from Steele et al. [59]. Copyright 2003 American Chemical Society)

and negative vectors (mass spectra) of an experimental analyte are compared with that of database spectra. A match occurs if both positive and negative vectors are within a 46° angle. If multiple standards match, then the closest negative ion spectrum match was considered as the experimental analyte. Positive spectra showed peaks <100 Da and negative spectra highlighted peaks <200 Da. Reproducibility depended strongly on laser wavelength and fluence. The wavelength of 266 nm was chosen because it was absorbed by dipicolinic acid (DPA) in the spores. The fluence or power was optimized to yield minimum variability from spectrum to spectrum. Spectral displays were averaged from 600 to 1000 particles. Different bacterial growth media for both spores saw minimal mass spectral differences within each species.

Determination of individual particles was made in real time in two steps. First, a prescreening stage eliminated nonbacterial particles by data analysis of the acquired spectra. The microbial-related spectra then went through mass-related criteria to refine and provide a database match to the experimental spectra. BG spores were identified 93.2% when compared to BT. Various commonly found and commercially available white powders were separately mixed with BG and BT to test the data analysis algorithm for interference properties. The spores recognized were as follows: 91% of the time with Gold Bond powder; 86% with growth media; 78% with Equal sweetener; 56% with fungal spores; and 46% with Knox gelatin [44].

Work then focused on efficient ionization characteristics of bacteria based on model biochemical compounds known to be found in bacteria [45]. Amino acids, DPA, and peptides were aerosolized and analyzed. Arginine and glycine amino acids are found in spore coats, and hence they were chosen as model compounds. A concern was the relative smallness of the particle compared to the laser beam cross-section. The cross-section of the beam fluence was not uniform, and the particles may have traveled through different areas of the cross-section, experiencing differential laser fluences. This was caused by the divergence of the particles as they travel through space. Thus, particles of the same size will have a similar divergence from the orifice.

Not all particles in an experiment produced a mass spectrum. Some percentage of the particles experience too wide a divergence from the laser beam, because some particles pass through a low-fluence region of the laser beam cross section. The highest effective ionization probability (EIP), or ratio of particles yielding spectra to the total number of particles, was approximately 40% for the biochemicals. DPA provided 35%, phenylalanine 31%, tryptophan had 30%, tyrosine had 23%, histidine had 20%, and arginine had 10%. The higher EIP substances have the UV absorbing aromatic side chains. Peptides were investigated and the one that had and did not have aromatic side chains yielded EIP values of 26% and <6%. As observed, an UV absorbing functional group in a compound provides a necessary avenue for ionization of the particle. This may be equivalent to the performance of a conventional MALDI organic matrix. Mixing a nonaromatic and an aromatic-containing compound together for bioaerosol analyses provided an increase in the EIP of the nonaromatic-containing compound. A MALDI-like effect

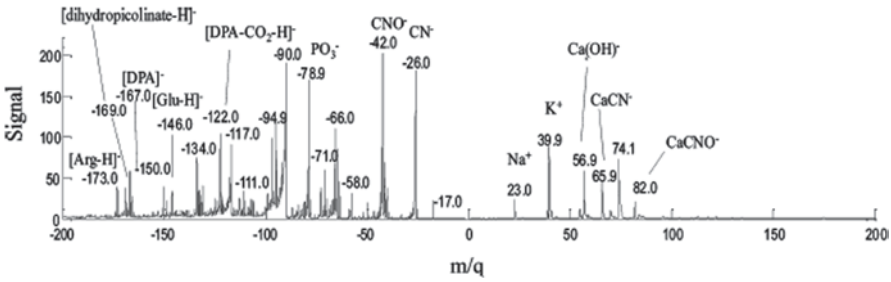

Fig. 9.11 Average of 1000 spectra of *Bacillus atrophaeus* spores using a dual-polarity time-of-flight mass spectrometer. (Reprinted with permission from Czerwieniec et al. [6]. Copyright 2005 American Chemical Society)

was suggested for these observations. Thus, acidities and basicities of the functional groups of particle analytes were shown to be important in the production of useable MS.

Isotope-Labeled Growth Media

Identification of substances is a very difficult task that produce peaks in a mass spectrum from the laser desorption/ionization of bacteria such as in BAMS, because any one particular peak usually arises from many compounds or fragments of larger compounds. An interesting analysis ensued where BG was grown in isotopically enriched media for targeting peaks in mass spectra of individual aerosol particles [6]. BG was grown until mid-log phase in regular media and then was transferred into either ^{15}N- or ^{13}C-labeled growth media. Growth proceeded until the stationary post-log phase was reached. Spectra were acquired in the positive and negative modes by TOF-MS. Figure 9.11 shows the nonlabeled media spectra of BG spores, comprising an average 1000 particle spectra. The dominant information was in the negative ion spectrum.

Major peaks were observed at m/z 167 and 166, which were tentatively identified as the molecular ion $(DPA)^-$ and $[M\text{-}H]^-$, respectively. A loss of CO_2 shows peaks at 123 and 122 for the pair of compounds. It is well known that DPA can comprise between 5 and 15% of the dry weight of a spore [5, 15, 29, 48]. A few other compounds are labeled, and Fig. 9.12a, b shows ^{15}N- and ^{13}C-labeled spectra, respectively. A number of peaks did not shift and are most notably the alkali and alkaline metal ions and their compounds as well as PO_3^{3-} when compared to Fig. 9.11. The DPA and DPA-CO_2 peaks shifted one mass unit higher. The arginine peak shifted four mass units higher because it contains four nitrogen atoms. The ^{15}N incorporation appeared complete in that there were was no mixture of labeled and unlabeled nitrogen-containing compounds. For ^{13}C-labeled bacterial aerosols, an envelope about each identified mass was observed and indicated only partial ^{13}C uptake in a percentage of the molecules in the spores. This phenomenon is observed

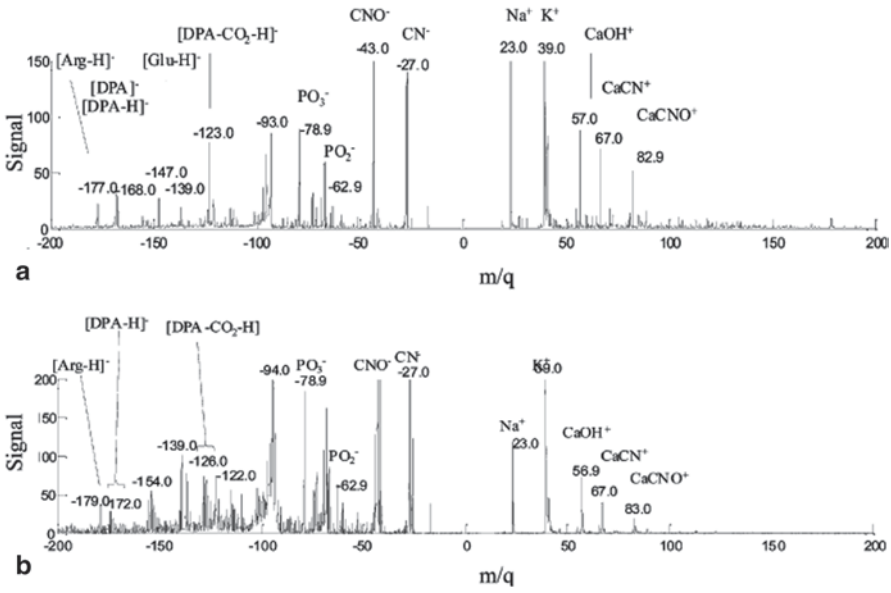

Fig. 9.12 (**a**) Average of 94 spectra of ^{15}N-labeled *B. atrophaeus* spores and (**b**) average of 28 spectra of ^{13}C-labeled spores using a dual-polarity TOF mass spectrometer. (Reprinted with permission from Czerwieniec et al. [6]. Copyright 2005 American Chemical Society)

in the $[DPA\text{-}H]^-$ and $[DPA\text{-}CO_2]^-$ peaks. The aerosol generation, spectral recording, and bacterial identity analysis occurred in the seconds' time frame.

A comprehensive identification of all major mass spectral peaks continued in a comparison of unlabeled BG aerosol spectra with that of the bacteria grown in ^{15}N- and ^{13}C-enriched media [58]. Fragments were also elucidated and standard biochemical aerosols were included to provide further confirmation of peaks. The compounds identified in the spectrum included metal ions, DPA, amino acids, trimethylglycine (betaine) and phosphate species, and the purine nucleobases adenine, guanosine diphosphate, and cytidine. These identified compounds from the BAMS system provide credibility that the pyrolyzed mass peaks seen at the <200 Da range are real and not artifacts of the pyrolysis event. These compounds are generally observed over a wide range of growth conditions since they are expected to be present in growing cells.

Sensitivity Parameter

Studies continued where an increase in sensitivity was addressed [46]. An updated BAMS system was constructed from the ion source, and ion guide wires were installed from the earlier version (Fig. 9.9). Initial testing used off-line MALDI by premixing matrix and analyte and impacting the particles on a plate for subsequent laser ionization. DHB was the matrix, and biochemicals such as gramicidin S, cy-

clodextrin, and carbohydrate molecules were used. Signals in the zeptomole concentration range were recorded.

Early in the BAMS technology it was observed that the laser fluence occupied a central position in the uniform ionization of particles and sensitivity issues. A concern was that the cross-section of the laser beam was inhomogeneous with respect to fluence or power [59]. Efforts were then made to provide a more uniform, flattened laser cross-section profile [60]. It was also observed that there was a minimum amount of power or fluence necessary to ablate, desorb, and ionize a particle. Many particles that passed through the laser cross-section were not ionized [59]. The explanation was that low-fluence regions in the laser cross-section existed, and particles did not experience enough energy for ionization. This in turn affected the reproducibility issue for a series of particles. Imperfectly focused aerosol particles are routine for an aerosol TOF-MS experiment and as such, different particles experienced different regions of a laser cross-section. This also affected the ability to identify a group of particles from a sample and resulted in differing amounts of energy absorbed by aerosol particles. BG and BT spores were investigated, and the hit rate was compared to laser pulse energy. The hit rate is the ratio of the number of particles producing spectra to the total number of particles. Laser energy vs. hit rate curve shows a 0.15 hit rate for 0.1 mJ laser pulse energy; a 0.125 mJ laser power yielded a 0.225 hit rate; and a >0.15 mJ laser power yielded a constant high hit rate of 0.25. A maximum of only 0.25 or 25 % of the particles produced spectra. Particles that were tracked by their time delay between two laser beams may have passed to the side of the 320 μm diameter of the downfield ionization laser beam and thus not experience the laser energy. The work stresses that proper laser fluence will yield a relatively flatter laser profile that produces better statistical particle identification.

Single Particle Aerosol Mass Spectroscopy

The BAMS evolved into the single-particle aerosol MS (SPAMS) system [61]. The suite of biological substances originally investigated was expanded to include chemical, biological, radiological, nuclear, and explosive (CBRNE) materials as well as clandestine/illegal drug substances. The SPAMS system used either two or three continuous wave laser beams to produce particle sizing properties. When a particle crosses the HeNe beam a light burst occurs that is captured by a detector. This allows for the particle's position, velocity, and aerodynamic diameter to be discovered. Three tracking lasers allowed for the evaluation of these three elements with high precision. The SPAMS could track up to 10,000 particles per second. The particle's position and velocity were used to predict when it passed through subsequent regions of the instrument. After the sizing region, the particle is interrogated by a laser-induced fluorescence region to determine the presence of UV fluorescence, which indicates biological nature. If the particle produced UV fluorescence, it was then ionized by a 266 nm laser beam. Identification of a particle occurred by mass spectral pattern matching with a database. Subsequent steps included selected ions (individual elements on a vector) which followed a rule tree. The angle between

a database vector (mass spectrum) and the experimental vector (a mass spectrum) was determined. Ubiquitous ions such as Na^+ and K^+ were removed. The closest angle match within certain limits was determined as the database vector identity.

The various substances produced significantly different experimental mass spectra, and no false identification or false alarms were observed with sequential challenges of the CBRNE materials. In addition to the analytes, there was a constant background of ambient outdoor particles such that the background particles dominated or were equivalent in temporal signal responses to the particular CBRNE challenge signals. Individual components of the mixture were RDX + cobalt to simulate a dirty bomb, RDX, and BG with no false alarms.

The SPAMS system was tested at the San Francisco, CA airport (SFO) and experienced varying environmental conditions over a 7-week time frame. The internal ambient atmosphere of the airport was sampled every minute, and the spectra were recorded. Approximately 1 million particles were tracked and recorded. After the recording and storage of the aerosol data, it was analyzed in the laboratory. No real-time analyses or decisions were made in the SFO field. In any 1-min interrogation, no more than two particles were identified as BG or pentaerythritol tetranitrate (PETN) explosive.

Off-Line Aerosol Analysis of Bacterial Biomarkers

Detection of Presence of Gram-Positive and -Negative Bacteria in Dust From Inherent Biochemicals

A series of papers by Fox and Larsson that are discussed in this section exemplify the difficulties and challenges that bioaerosols present. Their experiments attempted to find specific biochemical species in bacterial aerosols that allowed different stages of discrimination. These include trigger, detection, discrimination, and identification. However, these series of investigations dealt with absolute, not relative, determinations of specific biochemicals that are directly related to bacterial species. The aerosol samples were collected by an impactor in many outdoor and indoor scenarios. Off-line analyses took place in a laboratory where the fundamental systems were GC-MS and GC-tandem MS.

Organic dusts are found in the ambient environment and contain trace to ultratrace amounts of biological species including bacteria [64]. Agricultural environments contain organic dusts where a complex mixture of components includes feed components, dander, feathers, fecal material, pollen grains, insect parts, bacteria, and other bioactive materials. Bacteria in environmental locales can cause disease such as bronchitis, asthma, and airway hyperactivity of the lung regions. It is well known that a very low percentage (0.1–10 %) of bacteria in the environment can be observed by culture methods and that visual microscopy is limiting in identification information. These analytical methods were developed to search for chemical

markers that are unequivocal in origin in batch collected environmental aerosols. Analyses were performed off-line. Chemical markers constitute monomeric substances usually found covalently linked in the macromolecular architecture in a typical bacterium. Sample processing is such that the collected aerosol can remain on the filter. The entire sample was hydrolyzed to break up the macromolecular architecture into individual units. Purification by extraction was the next step and the selected monomers are derivatized to reduce the polarity of the functional groups such that the resulting compounds can pass through an analytical system such as a GC column with minimal loss.

Dust samples were collected in a room in a home and in a swine confinement building [47, 64]. Three distinct biochemical compounds were sought in the dust samples. Lipopolysaccharides (LPS) constitute a portion of the outer membrane of gram-negative bacteria and they contain unique chemical components. LPS causes challenges and insults to the human body, and they activate the immune system. Lipid A is the endotoxin component of LPS. It is responsible for endotoxicity and contains 3-hydroxy fatty acids (3-OH-FA). A comprehensive set of chemical reactions was performed to isolate the 3-OH-FA of the LPS material, and both dust samples were processed. The chemical steps culminate in the derivatization of the isolated 3-OH-FA species to reduce the polarity. Methyl esters are created and they are further derivatized with a trimethylsilyl reagent. GC-tandem MS was used to analyze for the derivatized 3-OH-FA. The mass spectra and tandem mass spectra of select precursor ions along with the GC retention times were matched to standard FA compounds. Unique swine and house dust GC patterns were observed, indicating a different gram-negative bacteria constitution at each locale. Specific FA and 3-OH-FA species were observed at the different places. The 3-OH-C14 FA was the most intense peak in the swine dust chromatogram, and the 3-OH-C16 FA was the most intense GC peak in the house dust chromatogram. These analyses showed the presence of gram-negative bacteria endotoxin (LPS) at a level of 0.01–0.094 nmol/mg of dust sample. Both dust samples were processed using another protocol to isolate ergosterol, which is found in the membranes of fungi and molds. GC-tandem MS showed very little of the chemical in the house dust, but a significant amount was observed in the swine dust. The low amount in the home environment indicates a relatively dry condition since molds thrive in damp conditions.

A third compound, muramic acid (Mur), is a nitrogen-containing carbohydrate found in the macromolecular peptidoglycan architecture [47, 64]. Peptidoglycan is found in gram-positive bacteria cell walls and is about 10× less in amount in gram-negative bacteria. Peptidoglycan is an immune system stimulant. A different procedure from the aforementioned methods was used to isolate Mur. Isolated Mur was derivatized and subjected to GC-MS analysis, and it was found in significant amounts in both dust samples.

A study was conducted by Lau et al. [37] in which sites in the greater Hong Kong area were subjected to sampling outdoor atmospheric aerosols. The objective was to investigate the presence of the fungal ergosterol chemical marker in the collected dust samples over a fall to spring 8-month time frame on a roughly weekly

schedule. Thus, one sample represented a week collection phase. The dust sample was processed to isolate ergosterol and it was derivatized for GC-MS analysis. Ergosterol was noted in amounts significantly more than the background levels in the October to December time region than that in the winter and spring months. The fall time frame saw amounts of ergosterol in the 200–400 pg/m^3 concentrations, while those in the winter and spring months averaged 100 pg/m^3.

Research led by Fox et al. [20] pioneered the concept of trace analysis of bacteria in ambient aerosol environments such as hospitals, farms, home locales, indoor company buildings, schoolrooms, and air duct vents in buildings. The key was to collect raw ambient aerosol samples and systematically use chemical and biochemical reactions to isolate specific and defined chemical monomers or components of the macromolecular architecture of gram-positive and gram-negative bacteria vegetative and spore cells as well as fungal/mold species. Specificity is relegated to the presence of either gram-positive or -negative organisms since that is what the procedure relates.

A very important concept in this research pioneered by Larsson was that samples were not subjected to liquid or solid growth media in flasks or Petri dishes. Almost 90% of ambient aerosols contain bacteria that do not grow on conventional microbiology media under controlled laboratory conditions. Thus, a vast amount of the bacterial load in the ambient atmosphere goes unaccounted. LPS includes L-, D-heptose, and 3-OH FA species. 3-OH dodecanoic acid (3-OH C12:0) and 3-OH tetradecanoic (3-OH C14:0) acids are the usual FA species in LPS which is exclusive to gram-negative cells. These two biochemicals, along with Mur from gram-positive peptidoglycan macromolecules, were investigated for their presence in the aerosol load in hospital air-conditioning systems.

The L-, D-heptose and Mur were analyzed by the alditol acetate technique [18, 19]. Further chemical reaction and processing methods were performed in order to isolate the derivatized compounds [20]. The 3-OH FAs were processed from the duct samples and resulted in methyltrimethylsilyl derivatives. All three isolated and derivatized biochemical species were analyzed by GC-MS. Results showed the presence of the biochemicals, which points to a contribution of gram-positive and gram-negative bacteria in the dust samples. Culturing techniques capture a small portion of the bacterial burden in an aerosol collection. Thus, biochemical and chemical methods were utilized directly on dust samples to extract and derivatize these three key biomarker compounds. Hospital air filters were investigated [21]. Air passed through a primary set of filters and was directed to a secondary set of filters found in the hospital rooms and hallways. The hospital and home filters were processed for the presence of gram-positive and gram-negative bacteria. The alditol acetate derivatization method was used to process the dust with GC-MS detection. The alditol acetate processing of Mur also removes interfering compounds [22]. Three ions characteristic of Mur were used, m/z 168, 404, and 446. Dust from the home and primary hospital filters were found to contain 26–31 ng of Mur per milligram of dust. The hospital secondary filters had about 5 ng/mg dust.

Shahgholi et al. [49] applied trace detection of chemical markers in environmentally collected barn dust aerosol samples with LC, ESI, tandem MS to tackle

the problem of Mur detection and identification. GC-MS detection necessitates a time-consuming alditol acetate derivatization procedure, which results in 53 h of processing. About 135 ng of Mur per milligram of hydrolyzed dust was observed with the liquid analysis method.

A study was performed by Krahmer et al. to investigate the Mur and 3-OH-FA levels in dust particulate in horse stable and dairy agricultural farm buildings by GC-tandem MS. It was shown that as the collected amount of dust increased, the amount of Mur and 3-OH-FA also increased. However, the least squares linear fit value for graphs on the amount of Mur in dust in a private horse stable and Mur in dust versus the dairy barn scenario were $r^2=0.98$ and 0.60, respectively. Product ion mass spectra of the precursor ion confirmed the presence of Mur. This study provided specific biomolecule measures that correlated with constant dynamic activity in the dairy scenario versus a relatively limited movement in the horse/animal stable.

Agar plate media only magnifies the viable bacterial portion of an aerosol; however, the Mur procedure measures both the viable and nonviable bacterial components. Impaction of aerosols onto an agar plate takes several seconds, and the plates were incubated for 24–48 h. In addition, the process of collecting dust on filters for biochemical analysis of Mur and 3-OH-FA requires 24–48 h. The total bacterial load in the aerosol from Mur determinations was much higher than that from agar plate counting techniques (Krahmer et al. 1998). This was in agreement with general knowledge in the area of bioaerosol analysis. Therefore, amounts of agricultural dust directly correlated with the amounts of Mur and 3-OH FA species. However, it is not straightforward to suggest that measuring the amount of dust in a bioaerosol would directly relate to the biological burden in the air. Rather, it may be viewed as complementary for an overall measure of the air bioburden.

A report by Pashynska et al. [43] collected ambient air particulate on quartz fiber filters in Ghent, Belgium. The carbohydrate-related compound levoglucosan was monitored. Levoglucosan is an anhydrous monosaccharide and is produced when cellulose-containing biomass substances are pyrolyzed, heated, or burned. Levoglucosan is a stable heating product. This compound was detected by isolation from a dust sample with trimethylsilylation for derivatization purposes. Other anhydrous monosaccharide compounds isolated from biomass burning were galactosan and mannosan. The glucose, arabitol, mannitol, fructose, and inositol sugars were also monitored. GC-ion trap tandem MS was used for detection and analysis. Dichloromethane (DCM), methanol (MeOH), and an 80 : 20 mixture of DCM-MeOH were used to test the extraction efficiency of the carbohydrate compounds from the untreated aerosol dust. The compounds are formed from burning biomass and may have adhered to the ambient particulate load. DCM and MeOH were determined to be effective solvents to extract the levoglucosan anhydrous monosaccharide from aerosol particulates. The MeOH and the DCM-MeOH solvent mixtures were effective in the extraction of levoglucosan and glucose. Galactosan and mannosan displayed relatively poor extraction efficiencies from all three solvents. All the extracted carbohydrates were then derivatized with trimethylsilyl reagent and

analyzed by GC-tandem MS. The compounds were clearly observed with comparisons to the respective standard compounds by GC retention time and mass spectral matching. Therefore, the collection of aerosols in winter and summer months [43] showed that the total amount of the anhydrous monosaccharide (levoglucosan) load in atmospheric particulates in the winter was greater than that in the summer. This correlates with the burning of wood. For the other carbohydrates (arabitol, mannitol, glucose, fructose, and inositol sugars), their amounts are relatively higher in summer than winter, because they arise from abundant vegetation particulates in the atmosphere.

A study was done to correlate the presence and levels of Mur, 3-OH FA, and CO_2 in two schools with different air-conditioning systems. A previous study [54] found that the amount of biomass, from the two biochemical markers, correlated with CO_2 levels in a direct manner. Thus, it was inferred that the organism load in the air in the school emanated from the children. The current work attempted to assess the chemical markers from the collected aerosol particulates and the CO_2 levels in occupied and unoccupied schoolrooms. Processing and analysis of the dust aerosol samples were similar to earlier studies, and GC-MS was used for detection. It was found that the chemical markers were considerably higher in the children-occupied versus unoccupied schoolrooms over defined periods of time. Mur was 6× higher in occupied versus unoccupied rooms, indicating differing levels of gram-positive organisms. The correlation of FA was more complex. C12 and C14 3-OH FAs were higher in occupied classrooms; C16 3-OH FA was lower in occupied versus unoccupied rooms; and the C10 3-OH FA was about the same in both types of rooms. This variability of 3-OH FA indicates that they originate from different types of gram-positive bacteria. In the earlier study [54], CO_2 levels mirrored that of the overall biomass. In this study, the airborne dust load, chemical marker amounts, and CO_2 levels yielded relatively higher amounts in occupied versus unoccupied classrooms. It was also suggested that the overall amount of gram-positive bacteria was higher than gram-negative bacteria in the classrooms based on the fact that Mur is found in both gram-positive and gram-negative bacteria, but that Mur is approximately 10× more abundant in gram-positive than gram-negative organisms. Another conclusion was that when children were not present a survey study of classrooms would underestimate the microbiological aerosol load.

Fox et al. continued investigations of the classroom indoor air quality with respect to the bacterial aerosol burden. Evidence strongly suggested that the presence of bacteria in the air in indoor schoolroom locales originated from the indoor environment and the building occupants. Analysis was then taken to a more sophisticated level. Instead of the determinations of bacterial compounds such as Mur and 3-OH FA species, the protein content of the collected aerosols was investigated. This takes the form of proteomics. Aerosol collection was performed as previously described previously. Total proteins were extracted from 50 to 100 mg dust and were processed. The purified protein mixture was separated using two-dimensional (2D) gel electrophoresis. Each protein spot was excised from the gel with subsequent isolation and purification procedures. These included dithreitol, iodoacetamide, trypsin digestion, and metal ion removal. The purified peptide mixture was

mixed with a MALDI matrix and MALDI-TOF-tandem MS was performed. Dust samples originating from occupied and unoccupied rooms were collected. The most abundant proteins from the gel-staining procedure were identified. One spot was more intense on the gels in both occupied and unoccupied rooms. MALDI-MS and MALDI-tandem MS identified the protein as human epithelial keratin K10. A standard sample also directly correlated with the experimental spot in gel electrophoresis comparisons and MALDI-MS procedures. This study showed that aerosol collection of indoor air indeed has a measurable quantity of human shed epithelial skin cells. Keratin was found to be the most abundant protein in airborne dust, and this was the first study to provide that information. The objective of bacterial protein studies evolved into an analysis of human proteins. These events took place due to the fact that human proteins dominated the gel electrophoresis studies.

Conclusions

MS techniques are providing applications and improvements to the analysis of bioaerosols in different settings. Improvements started after the initial utilization of pyrolysis MS, because versatility was added to the analysis of a wide range of cellular components in bioaerosol analyses. This versatility occurred by the advancement of desorption ionization MS techniques, which increased the detection capability for relatively large cellular components such as proteins and deoxyribonucleic acid (DNA). Desorption MS techniques faced challenges such as the need for a relatively large sample size to establish satisfactory detection limits and mass resolution. The greater the amount of sample, the higher the mass signal becomes for better figures of merit for a mass spectrum. However, the introduction of a reflectron TOF-MS system diminished those issues and enhanced the mass resolution. Alternatively, the sensitivity and bioaerosol collection efficiency were further improved with the introduction of an efficient aerodynamic lens and ion trap MS system, respectively. The latter technique provided attomole-level sensitivity for certain biochemicals in bacteria contained in 1 μm bioaerosol particles. Such developments were vital to bioaerosol analysis, because ion trap MS systems are portable, fieldable, and provide detection and identification in real-time scenarios.

Advancement in the field of MS analysis of bioaerosols was the introduction of an online TOF-MS system hybridized with spectroscopy techniques. This hybridization of optical fluorescence and mass determination technologies served as trigger and detector in one system. The first generation was scrutinized for mass resolution performance in single particle versus bulk analyses of bioaerosols. Engineering improvements in the hybridized TOF-MS system led to the development of the BAMS system. BAMS expanded the type of mass spectral information that could be obtained from biological samples in a single analysis by simultaneously collecting positive and negative ion mass spectra. Another improvement was the simultaneous recording of positive and negative ion mass spectra from the same bioaerosol particle for the first time. Moreover, BAMS eliminated the need for an

organic desorption matrix and provided analysis performance that matched conventional MALDI-MS techniques. Evolution of the BAMS led to the development of the SPAMS system. The SPAMS refined the BAMS technique and enhanced reproducibility through minimization of several hurdles such as the distribution of particle sizes and their effect on the laser beam triggers. The SPAMS expanded the application repertoire to the analysis of CBRNE aerosol materials.

Other significant studies that addressed the utilization of MS techniques in bioaerosol analysis were focused on finding biomarkers that were capable of discrimination of microbes present in indoor and outdoor environments in the literature of Larsson and Fox (*vide supra*). The importance of those studies relied on their ability to utilize mass spectral information to establish a comparative microbial profile to discriminate the origin of bioaerosols in environments such as in hospital, classroom, farm stable, or swine enclosures.

Overall, utilization of MS techniques in bioaerosol analysis has witnessed a steady development in the hardware, data processing tools, MS detectors, and range of applicability in real-time analysis scenarios. Such improvements and expansion in the type of information and diverse applications of MS techniques to bioaerosol detection and identification are advantageous. Those features position MS techniques as a forefront technology of choice for various bioaerosol applications. The continued improvement in the sensitivity of TOF-MS detectors combined with the cost-effectiveness of fieldable MS instruments is a factor that promises to provide value to the MS technology. The inherent complexity of bioaerosol contents and the emergence of environmental issues can be addressed with MS technologies by providing rapid detection and accurate identification of agents of interest to the public and private sectors.

Acknowledgements The authors wish to thank Mrs. Cynthia Swim and Mr. Alan Zulich and Dr. Vicky Bevilacqua for administrative and technical support.

References

1. Basile F, Voorhees KJ, Hadfield TL (1995) Microorganism Gram-type differentiation based on pyrolysis-mass spectrometry of bacterial fatty acid methyl ester extracts. Appl Environ Microbiol 61: 1534–1539
2. Basile F, Beverly MB, Abbas-hawks C, Mowry CD, Voorhees KJ, Hadfield TL (1998) Direct mass spectrometric evidence of in situ thermally hydrolyzed and methylated lipids from whole bacterial cells. Anal Chem 70: 1555–1562
3. Beeson MD, Murray KK, Russell DH (1995) Aerosol matrix-assisted laser desorption ionization: effect of analyte concentration and matrix-to-analyte ratio. Anal Chem 67:1981–1986
4. Bente M, Sklorz M, Streibel T, Zimmermann R (2009) Online laser desorption-multiphoton positionization mass spectrometry of individual aerosol particles: Molecular source indicators for particles emitted from different traffic-related and wood combustion sources. Anal Chem 81:4456–4467
5. Breed RS, Murray EGD, Smith NR (eds) (1957) Bergey's Manual of Determinative Bacteriology. The Williams and Wilkins Co., Baltimore, MD, 7th ed, pp 295–305.
6. Czerwieniec GA, Russell SC, Tobias HJ, Pitesky ME, Fergenson DP, Steele P, Srivastava A, Horn JM, Frank M, Gard EE, LeBrilla CB (2005) Stable isotope labeling of entire

Bacillus atrophaeus spores and vegetative cells using bioaerosol mass spectrometry. Anal Chem 77:1081–1087
7. de B Harrington P, Street TE, Voorhees KJ, Radicati di Brozolo F, Odom RW (1989) Rule-building expert system for classification of mass spectra. Anal Chem 61: 715–719
8. DeLuca S, Sarver EW, de B Harrington P, Voorhees KJ (1990) Direct analysis of bacterial fatty acids by Curie-point pyrolysis tandem mass spectrometry. Anal Chem 62: 1465–1472
9. DeLuca SJ, Voorhees KJ (1993) A comparison of products from an air atmosphere tube furnace with a vacuum Curie-point pyrolyzer: implications for biodetection. J Anal Appl Pyrolysis 24: 211–225
10. Dixon TC, Meselson M, Guillemin J, Hanna PC (1999) Medical progress: anthrax. N Engl J Med 341:815–826
11. Dongre AR, Eng JK, Yates III JR (1997) Emerging tandem-mass-spectrometry techniques for the rapid identification of proteins. Tibtech 15: 418–425
12. Dworzanski JP, Berwald L, Meuzelaar HLC (1990) Pyrolytic methylation-gas chromatography of whole bacterial cells for rapid profiling of cellular fatty acids. Appl Environ Microbiol 56: 1717–1724
13. Dworzanski JP, Berwald L, McClennen WH, Meuzelaar HLC (1991) Mechanistic aspects of pyrolytic methylation and transesterification of bacterial cell wall lipids. J Anal Appl Pyrolysis 21:221–232
14. Dworzanski JP, Snyder AP (2005) Classification and identification of bacteria using mass spectrometry-based proteomics. Expert Rev Proteomics 2: 863–878
15. Esposito AP, Talley CE, Huser T, Hollars CW, Schaldach CM, Lane SM (2003) Analysis of single bacterial spores by micro-Raman spectroscopy. Appl Spectrosc 57:868–871
16. Fei X, Wei G, Murray KK (1996) Aerosol MALDI with a reflectron time-of-flight mass spectrometer. Anal Chem 68:1143–1147
17. Fergenson DP, Pitesky ME, Tobias HJ, Steele PT, Czerwieniec GA, Russell SC, Lebrilla CB, Horn JM, Coffee, KR, Srivastava A, Pillai SP, Shih MTP, Hall HL, Ramponi AJ, Chang JT, Langlois RG, Estacio PL, Hadley RT, Frank M, Gard EE (2004) Reagentless detection and classification of individual bioaerosol particles in seconds. Anal Chem 76:373–378
18. Fox A, Morgan SL, Gilbart J (1989) Preparation of alditol acetates and their analysis by gas chromatography and mass spectrometry. In: Biermann CJ, McGinnis GD (eds) Analysis of Carbohydrates by GLC and MS. CRC Press, Boca Raton, FL, pages 87–117
19. Fox A, Black GE (1993) Identification and detection of carbohydrate markers for bacteria. Derivatization and gas chromatography-mass spectrometry. In: Fenselau C (ed) Mass Spectrometry for the Characterization of Microorganisms. American Chemical Society, Washington, DC, pages 107–131
20. Fox A, Rosario RMT, Larsson L (1993) Monitoring of bacterial sugars and hydroxyl fatty acids in dust form air conditioners by gas chromatography-mass spectrometry. Appl Environ Microbiol 59:4354–4360
21. Fox A, Rosario RMT (1994) Quantification of muramic acid, a marker for bacterial peptidoglycan, in dust collected from hospital and home air-conditioning filters using gas chromatography-mass spectrometry. Indoor Air 4:239–247
22. Fox A, Wright L, Fox K (1995) Gas chromatography-tandem mass spectrometry for trace detection of muramic acid, a peptidoglycan chemical marker, in organic dust. J Microbiol Methods 22:11–26
23. Gard E, Mayer JE, Morricai BD, Dienes T, Fergenson DP, Prather KA (1997) Real-time analysis of individual atmospheric aerosol particles: Design and performance of a portable ATOFMS. Anal Chem 69:4083–4091
24. Gieray RA, Reilly PTA, Yang M, Whitten WB, Ramsey JM (1997) Real-time detection of individual airborne bacteria. J Microbiol Methods 29:191–199
25. Griest WH, Wise MB, Hart KJ, Lammert SA, Thompson CV, Vass AA (2001) Biological agent detection and identification by the Block II chemical biological mass spectrometer. Field Anal Chem Technol 5: 177–184

26. Harris WA, Reilly PTA, Whitten WB (2005) MALDI of individual biomolecule-containing airborne particles in an ion trap mass spectrometer. Anal Chem 77:4042–4050
27. Hart KJ, Wise MB, Griest WH, Lammert SA (2000) Design, development, and performance of a fieldable chemical and biological agent detector. Field Anal Chem Technol 4: 93–110
28. Havey CD, Basile F, Mowry C, Voorhees KJ (2004) Evaluation of a micro-fabricated pyrolyzer for the detection of bacillus anthracis spores. J Anal Appl Pyrolysis 72: 55–61
29. Huang S-s, Chen D, Pelczar PL, Vepachedu VR, Setlow P, Li Y-q (2007) Levels of Ca^{2+}-dipicolinic acid in individual *Bacillus* spores determined using microfluidic Raman tweezers. J Bacteriol 189:4681–4687
30. Jackson SN, Murray KK (2002) Matrix addition by condensation for matrix-assisted laser desorption/ionization of collected aerosol particles. Anal Chem 74:4841–4844
31. Jackson SN, Mishra S, Murray KK (2004) On-line laser desorption/ionization mass spectrometry of matrix-coated aerosols. Rapid Commun Mass Spectrom 18:2041–2045
32. Kaufmann AF, Meltzer MI, Schmid GP (1997) The economic impact of a bioterrorist attack: are prevention and postattack intervention programs justifiable? Emerg Infect Diseases 3:83–94
33. Kim J-K, Jackson SN, Murray KK (2005) Matrix-assisted laser desorption/ionization mass spectrometry of collected bioaerosol particles. Rapid Commun Mass Spectrom 19:1725–1729
34. Kleefsman I, Stowers MA, Verhrijen PJT, van Wuijckhuijse AL, Kientz Ch E, Marijnissen JCM (2007) Bioaerosol analysis by single particle mass spectrometry. Part Part Syst Charact 24:85–90
35. Liu D-Y, Rutherford D, Kinsey M, Prather KA (1997) Realtime monitoring of pyrotechnically derived aerosol particles in the troposphere. Anal Chem 69:1808–1814
36. Liu H, Lin D, Yates III JR (2002) Multidimensional separations for protein/peptide analysis in the post-genomic era. BioTechniques 32: 898–911
37. Lau APS, Lee AKY, Chan CK, Fang M (2006) Ergosterol as a biomarker for the quantification of the fungi biomass in atmospheric aerosols. Atmospheric Environ 40:249–259
38. Mansoori BA, Johnston MV, Wexler AS (1996) Matrix-assisted laser desorption/ionization of size- and composition-selected aerosol particles. Anal Chem 68:3595–2601
39. Meuzelaar HLC, Windig W, Harper AM, Huff SM, McClennen WH, Richards JM (1984) Pyrolysis mass spectrometry of complex organic materials. Nature 226: 268–274
39. Meuzelaar HLC, Windig W, Harper AM, Huff SM, McClennen WH, Richards JM (1984) Pyrolysis mass spectrometry of complex organic materials. Nature 226: 268–274
40. Murray KK, Lewis TM, Beeson MD, Russell DH (1994) Aerosol matrix-assisted laser desorption ionization for liquid chromatography time-of-flight mass spectrometry. Anal Chem 66:1601–1609
41. Murray KK, Russell DH (1994a) Aerosol matrix-assisted laser desorption ionization mass spectrometry. J Am Soc Mass Spectrom 5:1–9
42. Murray KK, Russell DH (1994b) Liquid sample introduction for matrix-assisted laser desorption ionization. Anal Chem 65:2534–2537
43. Pashynska V, Vermeylen R, Vas G, Maenhaut W, Claeys M (2002) Development of a gas chromatographic/ion trap mass spectrometric method for the determination of levoglucosan and saccharidic compounds in atmospheric aerosols. Applications to urban aerosols. J Mass Spectrom 37:1249–1257
44. Ramponi AJ, Chang JT, Langlois RG, Estacio PL, Hadley RT, Frank M, Gard EE (2004) Reagentless detection and classification of individual bioaerosol particles in second. Anal Chem 7:373–378
45. Russell SC, Czerwieniec G, Lebrilla C, Tobias H, Fergenson DP, Steele P, Pitesky M, Horn J, Srivastava A, Frank M, Gard EE (2004) Toward understanding the ionization of biomarkers from micrometer particles by bio-aerosol mass spectrometry. J Am Soc Mass Spectrom 15:900–909
46. Russell SC, Czerwieniec G, Lebrilla C, Steele P, Riot V, Coffee K, Frank M, Gard EE (2005) Achieving high detection sensitivity (14 zmol) of biomolecular ions in bioaerosol mass spectrometry. Anal Chem 77:4734–4741

47. Sebastian A, Larsson L (2003) Characterization of the microbial community in indoor environments: a chemical-analytical approach. Appl Environ Microbiol 69:3103–3109
48. Setlow P J (2006) Spores of *Bacillus subtilis*: their resistance to radiation, heat and chemicals. Appl Microbiol 101:514–525
49. Shahgholi M, Ohorodnik S, Callahan JH, Fox A (1997) Trace detection of underivatized muramic acid in environmental dust samples by microcolumn liquid chromatography-electrospray tandem mass spectrometry. Anal Chem 69:1956–1980
50. Silva PJ, Prather KA (1997) On-line characterization of individual particles from automobile emissions. Environ Sci Technol 31:3074–3080
51. Sinha MP, Giffen CE, Norris DD, Estes TJ, Vilker VL, Friedlander SK (1982) Particle analysis by mass spectrometry. J Colloid Interface Sci 87:140–153
52. Sinha MP, Platz RM, Vilker VL, Friedlander SK (1984) Analysis of individual biological particles by mass spectrometry. Intl J Mass Spectrom Ion Processes 57:125–133
53. Sinha MP, Platz RM, Friedlander SK, Vilker VL (1985) Characterization of bacteria by particle beam mass spectrometry. Appl Environ Microbiol 49:1366–1375
54. Smedje G, Norback D (2001) Incidence of asthma diagnosis and self-reported allergy in relation to the school environment: A four-year follow-up study in schoolchildren. Intl J Tuberculosis Lung Dis. 5:1059–1066
55. Smith PB, Snyder AP (1993) Characterization of bacteria by oxidative and non-oxidative pyrolysis-gas chromatography/ion trap mass spectrometry. J Anal Appl Pyrolysis 24: 199–210
56. Snyder AP, Eiceman GA, Windig W (1988) Influence of pyrolytic techniques on mass spectra of biopolymers with chemical ionization at atmospheric pressure. J Anal Appl Pyrolysis 13: 243–257
57. Spurny KR (1994) On the chemical detection of bioaerosols. J Aerosol Sci 25:1533–1547
58. Srivastava A, Pitesky ME, Steele PT, Tobias HJ, Fergenson DP, Horn JM, Russell SC, Czerwieniec GA, Lebrilla CB, Gard EE, Frank RM (2005) Comprehensive assignment of mass spectral signatures from individual *Bacillus atrophaeus* spores in matrix-free laser desorption/ionization bioaerosol mass spectrometry. Anal Chem 77:3315–3332
59. Steele PT, Tobias HJ, Fergenson DP, Pitesky ME, Horn JM, Czerwieniec GA, Russell SC, LeBrilla CB, Gard EE, Frank M (2003) Laser power dependence of mass spectral signatures from individual bacterial spores in bioaerosol mass spectrometry. Anal Chem 75:5480–5487
60. Steele PT, Srivastava A, Pitesky ME, Fergenson DP, Tobias HJ, Gard EE, Frank M (2005) Desorption/ionization fluence thresholds and improved mass spectral consistency measured using a flattop laser profile in the bioaerosol mass spectrometry of single *Bacillus* endospores. Anal Chem 77:7448–7454
61. Steele PT, Farquar GR, Martin AN, Coffee KR, Riot VJ, Martin SI, Fergenson DP, Gard EE, Frank M (2008) Autonomous, broad-spectrum detection of hazardous aerosols in seconds. Anal Chem 80:4583–4589
62. Stowers MA, van Wuijckhuijse AL, Scarlett B, van Baar BLM, Klentz Ch E (2000) Application of matrix-assisted laser desorption ionization to on-line aerosol time-of-flight mass spectrometry. Rapid Commun Mass Spectrom 14:829–833
63. Su Y, Sipin MF, Furutani H, Prather KA (2004) Development and characterization of an aerosol time- of-flight mass spectrometer with increased detection efficiency. Anal Chem 76:712–719
64. Szponar B, Larsson L (2001) Use of mass spectrometry for characterizing microbial communities in bioaerosols. Ann Agric Environ Med 8:111–117
65. van Wuijckhuijse AL, Stowers MA, Kleefsman WA, van Baar BLM, Kientz Ch E, Marijnissen JCM (2005) Matrix-assisted laser desorption/ionisation aerosol time-of-flight mass spectrometry for the analysis of bioaerosols: development of a fast detector for airborne biological pathogens. J Aerosol Sci 36:677–687
66. Voorhees KJ, Harrington PB, Street TE, Hoffman S, Durfee SL, Bonelli JE, Firnhaber CS (1990) Approached to pyrolysis/mass spectrometry data analysis of biological materials. In: Meuzelaar HLC (ed) Computer-enhanced analytical spectroscopy. Modern analytical chemistry, vol 2. Plenum Press, New York, pp 259–275

67. Wilson KR, Jimenez-Cruz M, Nicolas C, Belau L, Leone SR, Ahmed M (2006) Thermal vaporization of biological nanoparticles: Fragment-free vacuum ultraviolet photoionization mass spectra of tryptophan, phenylalanine-glycine-glycine, and beta-carotene. J Phys Chem A 110:2106–2113
68. Windig W, Jakab E, Richards JM, Meuzelaar HLC (1987) Self-modeling curve resolution by factor analysis of a continuous series of pyrolysis mass spectra. Anal Chem 59: 317–323
69. Yates III JR (1998) Mass spectrometry and the age of the proteome. J Mass Spectrom 33: 1–19
70. Yates III JR (2004) Mass spectral analysis in proteomics. Annu Rev Biophys Biomed Struct 33: 297–316